



Contents lists available at ScienceDirect

Catalysis Today

journal homepage: [www.elsevier.com/locate/cattod](http://www.elsevier.com/locate/cattod)

## Activation pathways taking place at molecular copper precatalysts for the oxygen evolution reaction

Cornelis J.M. van der Ham<sup>a</sup>, Furkan Işık<sup>a</sup>, Tiny W.G.M. Verhoeven<sup>b</sup>, J.W. (Hans) Niemantsverdriet<sup>c</sup>, Dennis G.H. Hetterscheid<sup>a,\*</sup><sup>a</sup> Leiden Institute of Chemistry, Leiden University, 2300 RA Leiden, The Netherlands<sup>b</sup> Department of Chemical Engineering and Chemistry, Eindhoven University of Technology, P.O. Box 513, 5600 MB Eindhoven, The Netherlands<sup>c</sup> SynCat@DIFFER, Syngaschem BV, P.O. Box 6336, 5600 HH Eindhoven, The Netherlands

### ARTICLE INFO

#### Article history:

Received 7 September 2016

Received in revised form

19 December 2016

Accepted 21 December 2016

Available online xxx

#### Keywords:

Water oxidation

Copper oxide

Catalyst activation

### ABSTRACT

The activation processes of  $[\text{Cu}^{\text{II}}(\text{bdmpza})_2]$  in the water oxidation reaction were investigated using cyclic voltammetry and chronoamperometry. Two different paths wherein CuO is formed were distinguished.  $[\text{Cu}^{\text{II}}(\text{bdmpza})_2]$  can be oxidized at high potentials to form CuO, which was observed by a slight increase in catalytic current over time. When  $[\text{Cu}^{\text{II}}(\text{bdmpza})_2]$  is initially reduced at low potentials, a more active water oxidation catalyst is generated, yielding high catalytic currents from the moment a sufficient potential is applied. This work highlights the importance of catalyst pre-treatment and the choice of the experimental conditions in water oxidation catalysis using copper complexes.

© 2016 Published by Elsevier B.V.

### 1. Introduction

The water oxidation reaction is important to ensure future energy storage and sustainability. The reaction has been extensively studied in the presence of homogeneous water oxidation catalysts that predominantly are based on noble metals such as ruthenium [1–3] and iridium [4–9]. In particular in case of molecular ruthenium systems bearing bipyridine type ligands, mechanistic studies have provided the community with detailed insights how water oxidation catalysis occurs [10–12]. In case of other water oxidation catalysts the true active species turned out to be metal oxide deposits that were formed from their organometallic precursors under the harsh oxidative conditions applied [13–16]. In terms of atom abundance and economic viability, complexes that are based on first row transition metals are more interesting than their second and third row counterparts, albeit such systems typically don't operate well under acidic conditions. Due to substantial faster ligand dissociation kinetics at these first row transitions metals, control over the catalyst structure is considerably more cumbersome. Nevertheless, molecular catalysts in case of manganese [17], iron [18–20], cobalt [21] and since very recently copper [22–30] have been reported. Especially in case of the latter, lig-

and exchange kinetics are fast, and consequently several papers have appeared wherein copper oxides proved to be the competent catalytic species rather than their molecular precursors [31–35]. A fruitful strategy to prevent formation of copper oxides appears to lie with multi-denticity [29]. Nevertheless, also the copper bipyridine complexes, first reported by Mayer et al., appear to react exclusively *via* molecular sites [22,23], suggesting that discrimination between homogeneous *versus* heterogeneous catalysis is much more complex. From early cobalt polyoxometallate water oxidation chemistry the scientific community has already learned that the formation of which type of catalytic species is formed can be largely dependent on the exact reaction conditions applied, especially in case of highly dynamic systems [36–39].

Preliminary water oxidation studies in our lab in the presence of  $[\text{Cu}^{\text{II}}(\text{bdmpza})_2]$  ( $\text{bdmpza}^- = \text{bis}(3,5\text{-dimethyl-1H-pyrazol-1-yl})\text{acetate}$ , Fig. 1), a structure similar to the aforementioned copper bipyridine system, revealed that the observed water oxidation activity is strongly dependent on the electrochemical pretreatment of the molecular catalyst, even though the eventual catalytic experiments were carried out under the exact same conditions. In light of the discussion whether catalysis occurs at a homogeneous *versus* heterogeneous species and how one can control the activity of these catalytic species, the pretreatment dependence triggered us to investigate the catalyst activation pathways of  $[\text{Cu}^{\text{II}}(\text{bdmpza})_2]$  in detail. In this contribution we discuss two independent pathways to the formation of CuO, the true active

\* Corresponding author.

E-mail address: [d.g.h.hetterscheid@chem.leidenuniv.nl](mailto:d.g.h.hetterscheid@chem.leidenuniv.nl) (D.G.H. Hetterscheid).

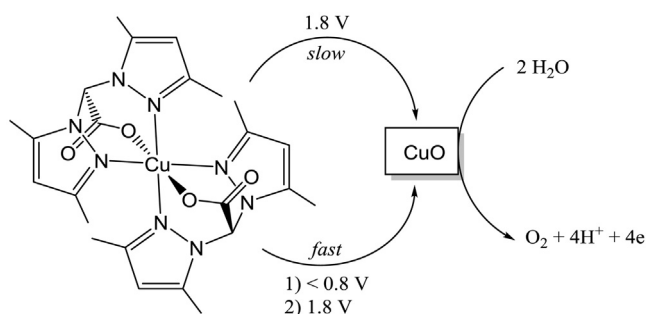


Fig. 1. Paths of activation observed for  $[\text{Cu}^{\text{II}}(\text{bdmpza})_2]$ .

species, wherein the observed reactivity is greatly activation path dependent.

## 2. Experimental

### 2.1. Complex synthesis

$[\text{Cu}^{\text{II}}(\text{bdmpza})_2]$  was obtained by dropwise addition of 0.33 mmol  $\text{bdmpzaNa}$  in 25 ml methanol to a solution of 0.33 mmol  $\text{Cu}^{\text{II}}(\text{OTf})_2$  in 25 ml methanol. After stirring for 30 min, part of the methanol was evaporated and diethyl ether was added to the reaction mixture to yield a blue-green precipitate overnight. The crystalline material was dried in vacuo and recrystallized from methanol at  $-20^\circ\text{C}$ , yielding  $[\text{Cu}^{\text{II}}(\text{bdmpza})_2]$ . The infrared spectra of  $[\text{Cu}^{\text{II}}(\text{bdmpza})_2]$  are in good agreement with previous reported data (see supporting info) [40]. ESI MS  $m/z$  (calc): 558.2 ( $[\text{M}]^+$ ), 580.2 ( $580.2, [\text{M}+\text{Na}]^+$ ), 612.2 ( $612.2, [\text{M}+\text{Na}+\text{MeOH}]^+$ ).

### 2.2. Electrochemical methods

All experiments were performed on an Autolab PGSTAT 128N. All electrochemical experiments were performed in one-compartment 25 ml glass cells in a three-electrode setup, using a gold working electrode (WE). In all cases a gold wire was used as a counter electrode and all experiments were measured against the reversible hydrogen electrode. The electrochemical cell was boiled twice in Millipore MilliQ water ( $>18.2\text{ M}\Omega\text{ cm}$  resistivity) prior to the experiment. The Au working electrode consisted of a disc and was used in a hanging meniscus configuration. The WE was cleaned by applying 10 V between the WE and a graphite counter electrode for 30 s in a 10%  $\text{H}_2\text{SO}_4$  solution. This was followed by dipping the WE in a 6 M HCl solution for 20 s. The electrode was flame annealed, followed by electrochemical polishing in 0.1 M  $\text{HClO}_4$ , while scanning between 0 and 1.75 V *versus* RHE for 200 cycles at  $1\text{ V s}^{-1}$ . Eventually  $5\ \mu\text{l}$  of a 18 mM solution of  $[\text{Cu}^{\text{II}}(\text{bdmpza})_2]$  in ethanol was dropcasted onto the working electrode and dried in air. The electrolyte solutions were prepared from MilliQ water ( $>18.2\text{ M}\Omega\text{ cm}$  resistivity) and  $\geq 99.9995\%$  NaOH obtained from Sigma-Aldrich.

The electrochemical quartz crystal microbalance (EQCM) experiments were performed in a 3 ml Teflon cell purchased from Autolab. As a working electrode, an Autolab EQCM electrode was used, wherein a 200 nm gold layer ( $1.5\text{ cm}^2$ ) was deposited on a quartz crystal. Since the hydrogen bubbles of the RHE reference electrode disturbed the frequency during the EQCM measurements, a  $\text{Pd}/\text{H}_2$  reference electrode was prepared by applying a potential of  $-4.0\text{ V}$  between the Pd wire and a platinum counter electrode for approximately 10 min. Prior to the experiment the potential of the  $\text{Pd}/\text{H}_2$  electrode relative to the RHE was determined. All EQCM data were corrected to the RHE scale. The sensitivity coefficient of the quartz crystal ( $c_f$ ) was determined by deposition

of  $\text{PbNO}_3$ . An electrolyte solution containing 10 mM  $\text{PbNO}_3$  and 0.1 M  $\text{HClO}_4$  was prepared. Cyclic voltammetry at  $100\text{ mV s}^{-1}$  gave the relationship between the  $\Delta f$  and the amount of Pb deposited onto the electrode. The sensitivity coefficient was determined to be  $1.26 \times 10^{-8}\text{ g cm}^{-2}\text{ Hz}^{-1}$  (Fig. S3). For the catalytic experiments,  $10\ \mu\text{l}$  of an 18 mM solution of  $[\text{Cu}^{\text{II}}(\text{bdmpza})_2]$  in ethanol was dropcasted onto the EQCM electrode, yet due to its geometry it was impossible to avoid that some  $[\text{Cu}^{\text{II}}(\text{bdmpza})_2]$  was deposited on the quartz part of the assembly. The actual amount of catalytic material that is in contact with the working electrode is therefore overestimated.

During the online electrochemical mass spectrometry (OLEMS) measurements the gaseous products formed at the working electrode were collected via a hydrophobic tip (KEL-F with a porous Teflon plug) in close proximity to the surface of the working electrode and analyzed in a Pfeiffer QMS 200 mass spectrometer. An Ivium A06075 potentiostat was used in combination with the OLEMS experiments. A detailed description of the OLEMS setup is available elsewhere [40].

### 2.3. XPS

XPS measurements were carried out with a Thermo Scientific K-Alpha, equipped with a monochromatic small-spot X-ray source and a  $180^\circ$  double focusing hemispherical analyzer with a 128-channel detector. Spectra were obtained using an aluminium anode ( $\text{Al K}\alpha = 1486.6\text{ eV}$ ) operating at 72 W and a spot size of  $400\ \mu\text{m}$ . Survey scans were measured at a constant pass energy of 200 eV and region scans at 50 eV. The background pressure was  $2 \times 10^{-8}$  mbar and during measurement  $4 \times 10^{-7}$  mbar Argon because of charge compensation.

Samples for XPS were prepared by chrono amperometry in 0.1 M NaOH at pH 13, using  $0.8\text{ cm}^2$  pyrolytic graphite discs as working electrodes. Prior to use, the electrodes were sanded with waterproof 2500 grit sandpaper. A total amount of 180 nmol  $[\text{Cu}^{\text{II}}(\text{bdmpza})_2]$  was dropcasted onto the electrodes and the discs were used in a hanging meniscus configuration.

## 3. Results

The  $\text{bdmpza}^-$  ligands of  $[\text{Cu}^{\text{II}}(\text{bdmpza})_2]$  are centrosymmetrically arranged around the copper ion, forming a *trans*- $\text{CuN}_4\text{O}_2$  complex, wherein the copper site is coordinatively saturated [41]. However, it is not unprecedented that one of the ligand arms of  $\text{bdmpza}^-$  dissociates in favor of coordination of water [42], providing an entry into catalysis at a molecular species. The redox chemistry of  $[\text{Cu}^{\text{II}}(\text{bdmpza})_2]$  was explored by dropcasting the complex onto a gold working electrode (WE). Fig. 2 shows the cyclic voltammogram of 90 nmol  $[\text{Cu}^{\text{II}}(\text{bdmpza})_2]$  dropcasted onto a  $0.050\text{ cm}^2$  (geometric surface area) gold electrode in a 0.1 M aqueous NaOH solution at pH 13. The experiment was started at 1.2 V *versus* RHE and scanned towards positive potentials initially. In the first scan relatively little catalytic current is observed, which contrasts the second and third scans. Scanning the potential up to 2.0 V *versus* RHE resulted in a small peak (designated 1 in Fig. 2) in the cyclic voltammogram, which does not exceed the current displaying that of a blank gold electrode under the same conditions (see Fig. S4). While starting above 1.2 V *versus* RHE and scanning into a positive direction first or scanning in negative direction immediately does not result in changes in the reduction chemistry. Below 1.2 V a series of sharp reduction peaks (2–5 in Fig. 2) can be observed that lie on top of a broad negative baseline current that starts roughly at 0.8 V *versus* RHE. The negative baseline current continues upon scanning into the positive direction until 0.8 V after which a very sharp oxidative peak (7) is observed at 0.9 V *versus* RHE.

Download English Version:

<https://daneshyari.com/en/article/4756912>

Download Persian Version:

<https://daneshyari.com/article/4756912>

[Daneshyari.com](https://daneshyari.com)